

## Superdeformation below $N=73$

A. Galindo-Uribarri,<sup>1</sup> S. M. Mullins,<sup>2,\*</sup> D. Ward,<sup>1</sup> M. Cromaz,<sup>3</sup> J. DeGraaf,<sup>3</sup> T. E. Drake,<sup>3</sup> S. Flibotte,<sup>2,†</sup> V. P. Janzen,<sup>1</sup>  
D. C. Radford,<sup>1</sup> and I. Ragnarsson<sup>4</sup>

<sup>1</sup>AECL, Chalk River Laboratories, Chalk River, Ontario, Canada K0J 1J0

<sup>2</sup>Department of Physics and Astronomy, McMaster University, Hamilton, Ontario, Canada L8S 4M1

<sup>3</sup>Department of Physics, University of Toronto, Toronto, Ontario, Canada M5S 1A7

<sup>4</sup>Department of Mathematical Physics, Lund Institute of Technology, P.O.Box 118, S-221 00 Lund, Sweden

(Received 26 March 1996)

A decoupled rotational band with an average dynamical moment of inertia  $\mathcal{J}^{(2)} \sim 55 \hbar^2/\text{MeV}$  has been observed to high spin in  $N=71$   $^{129}\text{Ce}$ . The measured quadrupole moment of  $Q_0 = 6.3(4)$  eb is as large as that of the superdeformed band in  $^{131}\text{Ce}$ . The large deformation and decoupled character of the band suggests that the odd neutron occupies either the  $h_{9/2}/f_{7/2}$  [541]  $1/2^-$  orbital or the  $i_{13/2}$  [660]  $1/2^+$  intruder orbital. This is the first example of a superdeformed band extending to high spin below  $N=73$ , a neutron number that has long been considered as the boundary for superdeformation in the  $A \sim 130$  mass region. [S0556-2813(96)50308-0]

PACS number(s): 27.60.+j, 23.20.Lv, 21.10.Re, 21.60.Ev

The occurrence of strongly-deformed nuclear shapes has opened up a vigorous debate concerning the relative importance of “core stabilization” from shell gaps (or particle-hole excitations within the system of normal-parity states), versus “core polarization” attributed to the occupancy of unique-parity valence intruder orbitals.<sup>1</sup> As we will show, there is an increasing body of evidence that the former mechanism is the more important, and that the appearance of the intruder states is mainly a consequence of, rather than the major contributor to, the deformation. This is not to preclude small adjustments of the nuclear mean field in excited configurations that include intruder orbitals.

Many examples of strongly-deformed shapes occur in the  $A=130$  mass region, where for a number of years experimental results were consistent with the assertion that the occupancy of the  $i_{13/2}$  neutron intruder orbital polarizes the nucleus to prolate deformations of  $\beta_2 \approx 0.3-0.4$ , often called superdeformed. Since the occupancy of the first  $i_{13/2}$  intruder orbital is energetically unfavored below neutron number  $N=73$ , it was believed [3] that structures with deformations as large as those of the  $\nu i_{13/2}$  bands could not occur at low excitation energy and hence be observable in nuclei with  $N < 73$ . Stabilization of superdeformed shapes in the  $A \sim 130$  region was thought to depend much less on shell gaps than it did in other regions of superdeformation. This belief was called into question by a recent study of  $^{131}\text{Pr}$  [4] that revealed a strongly-coupled band that was interpreted as a single-quasiproton structure based on the [404]  $9/2^+$  orbital but which has a deformation of  $\beta_2 = 0.35$ , a value typical of superdeformed bands in the  $A=130$  region. The low spin and excitation energy of the bandhead suggested that the  $i_{13/2}$  neutron intruder orbital was not occupied. These characteristics suggest that in this nucleus, the superdeformed shape is stabilized by the large energy gaps present in the

Nilsson diagram at  $Z=58$  (created by a proton hole in the [404]  $9/2^+$  orbital) and  $N=72$ . Furthermore, we have now deduced [5,6] that similar strongly-coupled bands in  $^{129}\text{Pr}$  [7] and  $^{133}\text{Pm}$  [8], are also based on strongly-deformed [404]  $9/2^+$  configurations. Thus, there are presently three examples of “core-stabilized,” superdeformed, low-spin [404]  $9/2^+$  bands in odd- $Z$  even- $N$  nuclei. Here we report on the observation of a high-spin decoupled rotational band in  $^{129}\text{Ce}$  ( $N=71$ ) for which lifetime measurements indicate a deformation as large as that of the superdeformed band in  $^{131}\text{Ce}$ .

The experiments were performed with the  $8\pi$   $\gamma$ -ray spectrometer, which is located at the TASCC facility of the Chalk River Laboratories of AECL. The  $8\pi$  spectrometer consists of an array of twenty Compton-suppressed hyperpure germanium (HPGe) detectors coupled with a bismuth germanate (BGO) calorimeter of seventy-one elements. A beam of  $^{28}\text{Si}$  ions was provided at an energy of 125 MeV by the upgraded MP tandem accelerator of the TASCC facility. The beam was directed onto a target that, in the first experiment, consisted of a stack of two  $\sim 600 \mu\text{g}/\text{cm}^2$  foils enriched to  $\sim 98\%$  in  $^{104}\text{Pd}$ . States in  $^{129}\text{Ce}$  [9] were populated in the  $2pn$  exit channel. In the second experiment the target consisted of a  $780 \mu\text{g}/\text{cm}^2$   $^{104}\text{Pd}$  foil mounted on a 17 mg/cm<sup>2</sup> Pb backing. The purpose here was to measure mean lifetimes with the Doppler-shift attenuation method (DSAM). The same event trigger was employed in both experiments, namely a prompt HPGe-HPGe-calorimeter coincidence, where a minimum of seven BGO elements had to fire. The energies of coincident pairs of  $\gamma$  rays detected in the HPGe array were recorded onto magnetic cassette, as were the number of BGO elements that fired (the “fold,”  $K$ ) and the total energy deposited (the “sum-energy,”  $H$ ). Energy and relative efficiency calibrations of the HPGe detectors were obtained with  $^{152}\text{Eu}$  and  $^{133}\text{Ba}$  sources.

The data obtained with the self-supporting target were sorted into an  $E_\gamma$ - $E_\gamma$  coincidence matrix under the condition that the sum energy recorded in the BGO ball was  $\geq 18$  MeV. This greatly enhanced the fraction of 3-particle exit channels over those in which 4 particles were evaporated. Analysis of the coincidence matrix was performed with the code Esc18r from the RADWARE [10] suite of programs. The

\*Present address: Department of Nuclear Physics, RSPHysSE, The Australian National University, Canberra, ACT 0200, Australia.

†Also AECL, Chalk River Laboratories, Chalk River, ON Canada KJO 1J0.

<sup>1</sup>See, for example, Refs. [1,2] and references therein.

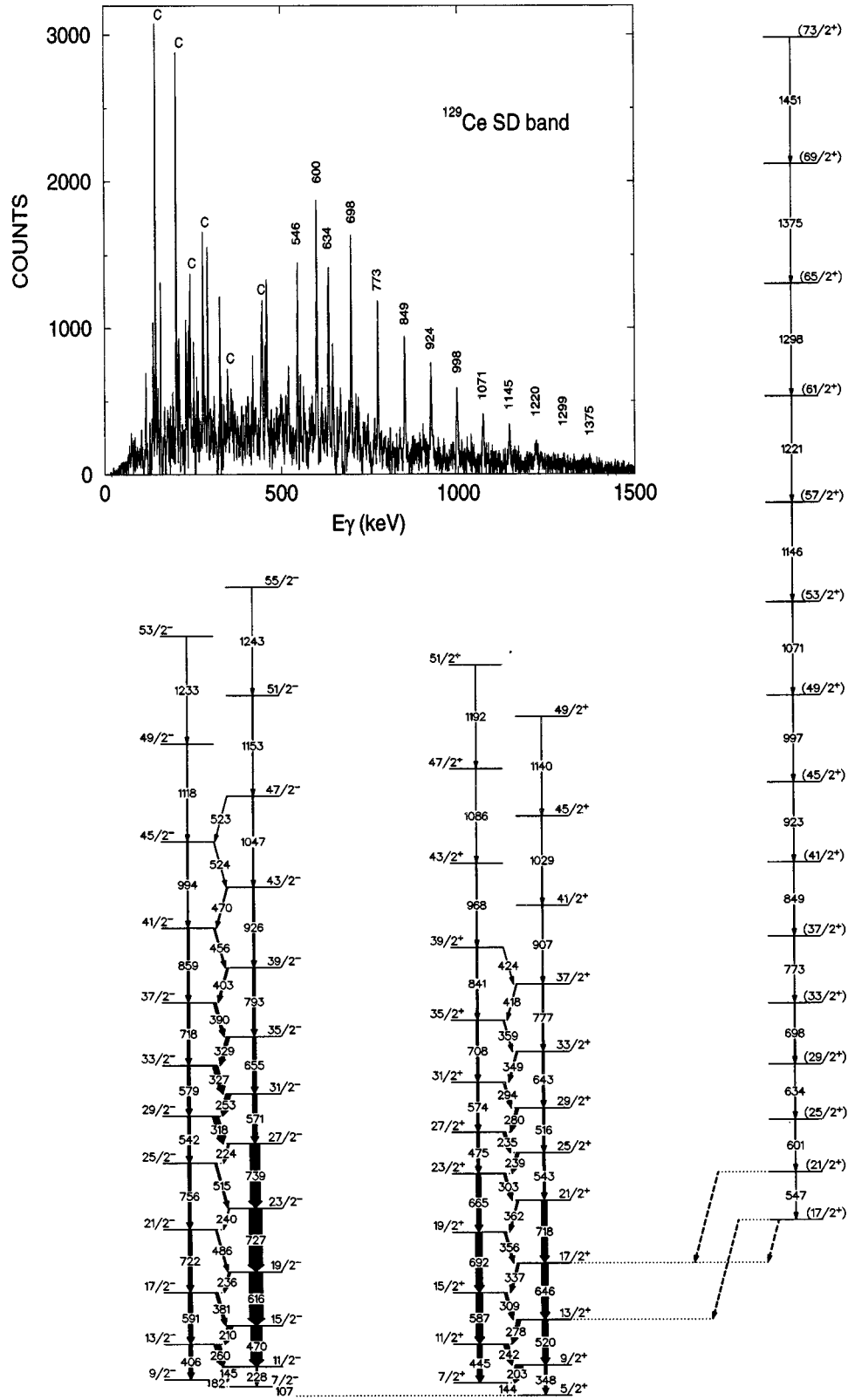


FIG. 1. Partial level scheme for  $^{129}\text{Ce}$ . The width of each arrow is proportional to the coincidence intensity for the respective transition. Inset: summed coincidence spectrum of the decoupled band in  $^{129}\text{Ce}$ . The energies of the transitions in the superdeformed band are given in keV. Transitions in the “normal”  $[402] 5/2^+$  band are identified with a “C.”

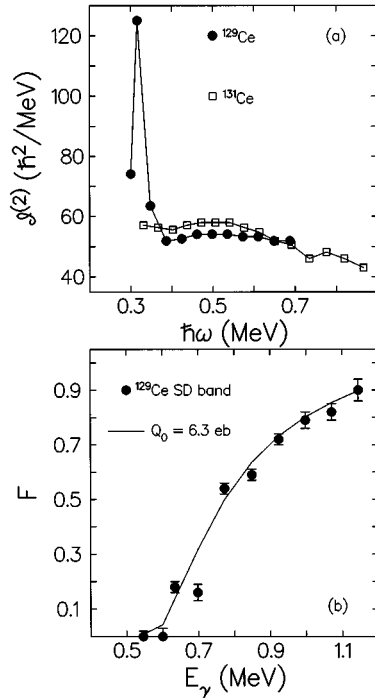


FIG. 2. (a)  $\mathcal{J}^{(2)}$  dynamic moments versus rotational frequency for the SD bands in  $^{129}\text{Ce}$  and  $^{131}\text{Ce}$ . (b) Centroid-shift data and calculated fits for the SD band in  $^{129}\text{Ce}$ .

two previously known strongly-coupled bands in  $^{129}\text{Ce}$  [9], based on the  $[402] 5/2^+$  and  $[523] 7/2^-$  Nilsson orbitals, were extended to higher spin. A new decoupled band was found and assigned to  $^{129}\text{Ce}$  through coincidences with known transitions in the  $[402] 5/2^+$  band, but no discrete linking transitions could be found. The intensity of this band was found to be 1.7% of the total intensity of the two

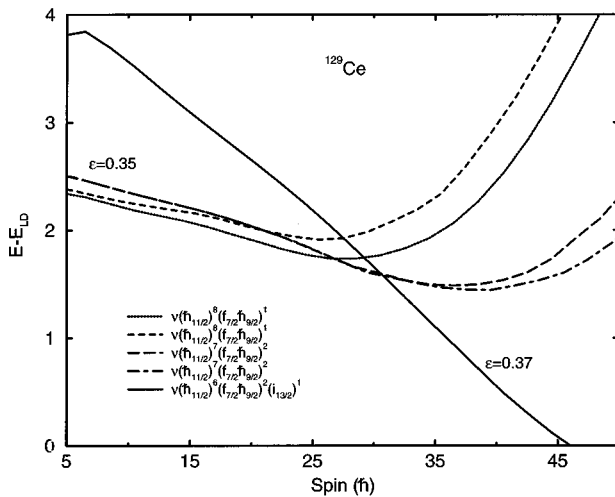


FIG. 3. Self-consistent diabatic Nilsson model calculations for various highly deformed neutron configurations in  $^{129}\text{Ce}$ . The configurations are labelled by the number of particles in the high- $j$  orbitals of the  $N=5$  ( $h_{11/2}$ ) and  $N=6$  ( $i_{13/2}$ ) shells and in the  $f_{7/2}/h_{9/2}$  subshell. All bands shown are ‘‘pushed’’ to large deformation by two holes in the upsloping  $[404] 9/2$  proton orbital creating a large  $Z=58$  shell gap at large deformation.

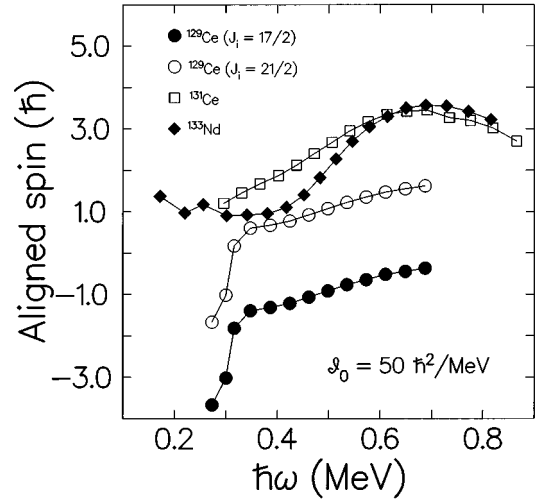


FIG. 4. Aligned spins for the SD bands in  $^{129}\text{Ce}$ ,  $^{131}\text{Ce}$ , and  $^{133}\text{Nd}$ .

strongly-coupled bands. These structures are shown in the partial level scheme presented in Fig. 1. The aforementioned coincidence relationships are consistent with an assignment of  $(17/2 \pm 2)\hbar$  to the lowest observed level of the decoupled band. For reasons to be discussed below, an assignment of  $17/2$  or  $21/2\hbar$  is favored. The spectrum of the decoupled band shown inset in Fig. 1 was generated from summing gates set on the 12 transitions from 546 to 1299 keV.

The  $\mathcal{J}^{(2)}$  moment of inertia was extracted by taking differences between the energies of successive transitions. It is shown as a function of rotational frequency in Fig. 2(a), and compared with  $\mathcal{J}^{(2)}$  values for the superdeformed band in  $^{131}\text{Ce}$  [11]. Clearly the  $\mathcal{J}^{(2)}$  values of the two bands are similar, which suggests that they may be based on states of similar deformation. Nuclear deformation may be inferred from lifetime measurements, and such measurements have been published for  $^{131}\text{Ce}$  [12]. In the present work, the highly-deformed character of the band in  $^{129}\text{Ce}$  was confirmed from a DSAM analysis of the Pb-backed target data. The 547 and 601 keV transitions were found to have decayed after the recoiling  $^{129}\text{Ce}$  nuclei had come to rest in the backing. These lines were used as gating transitions to project two spectra, one for events in which a detector at  $37^\circ$  fired, and a similar one for  $143^\circ$ . Centroid shifts were determined from these two spectra and were converted to the fractional shifts, or  $F$  values, shown in Fig. 2(b). Data for the high-spin members of the ‘‘normal-deformed’’  $[402] 5/2^+$  band were also processed. The fitted curves were generated under the assumption of decay down a single rotational band of constant quadrupole moment. The slowing down of the recoiling ions was modelled with the electronic stopping powers of Northcliffe and Schilling [13], scaled with the  $\alpha$  stopping powers of Ziegler and Chu [14]. Nuclear stopping and scattering were treated with the LSS/Blaugrund [15,16] formalism. A best-fit value of quadrupole moment  $Q_0 = 6.3(4)$  eb was obtained for the superdeformed band, whereas the ‘‘normal-deformed’’  $[402] 5/2^+$  band gave a result of  $Q_0 = 3.5(5)$  eb. A value of  $Q_0 = 6.3(4)$  eb had been extracted for  $^{131}\text{Ce}$  with the same analysis procedure [17]. Very recently a value of  $Q_0 = 7.4(3)$  eb has been reported in Ref. [18]. For both measurements the absolute values do not include sys-

tematic errors from uncertainties in the stopping powers which can be 15%.

Thus, the DSAM results clearly indicate that the bands in  $^{129}\text{Ce}$  and  $^{131}\text{Ce}$  have similar deformations of  $\beta_2 \approx 0.35$  [19]. Hence, the band in  $^{129}\text{Ce}$  represents the first observation of a high-spin superdeformed structure in a nucleus below  $N=73$  in the  $A=130$  mass region.

The large deformation and decoupled character of the band limit the possibilities of the orbital occupied by the odd neutron to either the  $h_{9/2}/f_{7/2}$ [541]  $1/2^-$  or the  $i_{13/2}$  [660]  $1/2^+$  Nilsson states and we now discuss the relative merits of these two candidates. They are the only  $\Omega = 1/2$  orbitals predicted to be near the Fermi surface for  $\beta_2 \sim 0.35$  in either a Woods-Saxon or a Nilsson model calculation. The  $h_{9/2}/f_{7/2}$  assignment is preferred, since both models predict that the  $i_{13/2}$  intruder lies  $\sim 2$  MeV higher in excitation energy in a static potential. Under the influence of rotation, the  $i_{13/2}$  orbital is brought down rapidly due to its large aligned spin, but unpaired cranking calculations suggest that the  $h_{9/2}/f_{7/2}$  orbital remains lowest (see, for example, Fig. 21 of Ref. [20].) In Fig. 3 are shown our unpaired Nilsson model calculations, in which the energy was minimized self-consistently with respect to the  $(\varepsilon_2, \varepsilon_4, \gamma)$  set of deformation parameters. Highly deformed configurations in  $^{129}\text{Ce}$ , characterized by two proton holes in the [404]  $9/2$  orbital, have been followed diabatically as a function of spin. The calculations predict that a band based on the  $i_{13/2}$  intruder orbital becomes favored over the lowest  $h_{9/2}/f_{7/2}$  configuration at spins beyond  $\sim 30 \hbar$ . Hence, the relatively low input angular momentum of the  $^{129}\text{Ce}$  reaction ( $l_{\text{max}} \sim 35 \hbar$ ) would appear to disfavor the  $i_{13/2}$  assignment. It should be noted, however, that it was possible to populate superdeformed bands in  $^{131}\text{Ce}$  ( $N=73$ ) and  $^{135}\text{Nd}$  ( $N=75$ ) with  $^{18,16}\text{O}$ -induced reactions, in which  $l_{\text{max}} \sim 30-35 \hbar$  [21]. In these cases, the intruder was predicted to be close to the Fermi level, making it easier to populate these bands in low- $l$  reactions.

It would be straightforward to distinguish between the two configurations if the parity of the band in  $^{129}\text{Ce}$  were known. The coincidences observed with the lower members of the positive-parity [402]  $5/2^+$  band may be construed as evidence that the superdeformed band has positive parity, since the decay-out could result from mixing between states of the same spin and parity. For example, the decay-out of the superdeformed band in  $^{133}\text{Nd}$  [22] is initiated by mixing between its members and  $N_{\text{osc}}=4$  states of normal deformation. The rapid rise in the  $\mathcal{J}^{(2)}$  dynamic moment of  $^{129}\text{Ce}$  at  $\hbar\omega \approx 0.28$  MeV could be due to a perturbation of the lower states by such mixing. Similar behavior is seen in many of  $\mathcal{J}^{(2)}$  values in odd- $N$  superdeformed bands in the  $A \sim 130$  region.

Since both orbitals ( $h_{9/2}/f_{7/2}$  and  $i_{13/2}$ ) have the same favored signature of  $\alpha = +1/2$  they will give rise to the same spin sequence, which rules out the assignment of  $15/2$  or  $19/2$  to the lowest observed level in the band. In principle, a comparison of the aligned spins of superdeformed bands in  $^{129}\text{Ce}$  and  $^{131}\text{Ce}$  should aid with the assignment, since the aligned spin of the  $h_{9/2}/f_{7/2}$  orbital will be  $\sim 2 \hbar$  less than that of the  $i_{13/2}$  orbital. Unfortunately, the spins of the band members are not known in either nucleus. Notwithstanding, a comparison can be made under the assumption that the lowest observed superdeformed level in  $^{129}\text{Ce}$  has a spin of  $17/2$  or  $21/2 \hbar$ , while a value of  $29/2 \hbar$  has been taken for  $^{131}\text{Ce}$ . The latter value has been assumed from comparison with its isotone  $^{133}\text{Nd}$ , for which spins have been established [22]. The aligned spins for all three bands are shown in Fig. 4 relative to a frequency-independent reference parametrized by  $\mathcal{J}_0 = 50 \hbar^2/\text{MeV}$ . The smooth rise observed in  $^{131}\text{Ce}$  and  $^{133}\text{Nd}$  is probably due to the alignment of the first pair of  $h_{11/2}$  protons, although cranking calculations are unable to reproduce either the smoothness of the crossing, or the small gain ( $\Delta i_x \approx 2 \hbar$ ) in aligned spin. This failure has been taken as evidence for a strong residual interaction between the aligning protons ( $h_{11/2}$ ) and neutrons ( $i_{13/2}$ ) [23]. If the odd neutron occupies the  $h_{9/2}/f_{7/2}$  orbital, then the residual interaction is expected to be weaker [24], and the proton  $h_{11/2}$  crossing should be sharper, i.e., in better agreement with cranked mean-field calculations. It is possible that the abrupt increase of aligned spin in  $^{129}\text{Ce}$  at  $\hbar\omega \approx 0.3$  MeV is due to the  $h_{11/2}$  proton crossing, thus providing supporting evidence that the band is not based on the  $i_{13/2}$  intruder, since the crossing frequency is close to that predicted by the cranked shell model for the  $h_{11/2}$  proton alignment. Moreover, it is interesting to note that at  $\hbar\omega \approx 0.7$  MeV, where the  $h_{11/2}$  protons appear to be maximally aligned in  $^{131}\text{Ce}$  and  $^{133}\text{Nd}$  (as they already are assumed to be in  $^{129}\text{Ce}$ ), the aligned spin in the  $21/2 \hbar$  assignment to  $^{129}\text{Ce}$  is  $\sim 2 \hbar$  lower, as would be expected for a  $\nu h_{9/2}/f_{7/2}$  assignment.

In conclusion, we have discovered a rotational band in  $^{129}\text{Ce}$  that has similar  $\mathcal{J}^{(2)}$  dynamic and quadrupole moments to the superdeformed band known in  $^{131}\text{Ce}$ . These characteristics indicate that this is the first observation of a high-spin superdeformed band in a nucleus below  $N=73$  in the  $A=130$  region. The decoupled character and enhanced deformation of the band limit the possibilities of the orbital that is occupied by the odd neutron to either the  $h_{9/2}/f_{7/2}$  [541]  $1/2^-$  orbital or the  $i_{13/2}$  [660]  $1/2^+$  intruder orbital. Proton holes in the [404]  $9/2$  orbital play an important role in stabilizing the shape at large deformation.

This work was supported by the Natural Sciences and Engineering Research Council of Canada, AECL, the Swedish Natural Sciences Research Council, and the Nordic Council of Ministers.

- 
- [1] T. R. Werner, J. Dobaczewski, M. W. Guidry, W. Nazarewicz, and J. A. Sheikh, Nucl. Phys. **A578**, 1 (1994).  
 [2] All articles in Int. J. Mod. Phys. E **2** (1993).  
 [3] R. A. Wyss, A. Johnson, W. Nazarewicz, and J. Nyberg, Phys. Lett. B **215**, 211 (1988).

- [4] A. Galindo-Uribarri *et al.*, Phys. Rev. C **50**, R2655 (1994).  
 [5] A. Galindo-Uribarri *et al.*, Report No. AECL-11132, PR-TASCC-09 (1994).  
 [6] A. Galindo-Uribarri *et al.*, Phys. Rev C (to be published) (Report No. TASCC-P-96-6).

- [7] A. N. James and D. C. B. Watson, in *Nuclei Far From Stability*, Proceedings of the International Conference, Lake Rosseau, Ontario, 1988, AIP Conf. Proc. No. 164, edited by I. S. Towner (AIP, New York, 1988), p. 425.
- [8] P. H. Regan *et al.*, Nucl. Phys. **A533**, 476 (1991).
- [9] R. Aryaeinejad, D. J. G. Love, A. H. Nelson, P. J. Nolan, P. J. Smith, D. M. Todd, and P. J. Twin, J. Phys. G. **10**, 955 (1984).
- [10] D. C. Radford, in *Proceedings of the International Seminar on the Frontier of Nuclear Spectroscopy*, Kyoto, Japan, 1992, edited by Y. Yoshizawa, H. Kusakari, and T. Otsuka (World Scientific, Singapore, 1993), p. 229; and Nucl. Instrum. Methods A **361**, 297(1995).
- [11] Y-X. Luo *et al.*, Z. Phys. **A329**, 125 (1988).
- [12] Y-J. He *et al.*, J. Phys. G. **16**, 657 (1990).
- [13] L. C. Northcliffe and R. F. Schilling, Nucl. Data Tables **A7**, 233 (1970).
- [14] J. F. Ziegler and W. K. Chu, At. Data Nucl. Data Tables **13**, 463 (1974).
- [15] J. Lindhard, M. Scharff, and H. E. Schift, K. Dan. Vidensk. Selsk. Mat. Fys. Medd. **33**, 14 (1963).
- [16] A. E. Blaugrund, Nucl. Phys. **88**, 173 (1966).
- [17] D. Ward *et al.*, in *Proceedings of the Conference on Physics from Large  $\gamma$ -Ray Detector Arrays*, Berkeley Laboratory, 1994, Vol. 1, p. 4.
- [18] R. M. Clark *et al.*, Phys. Rev. Lett. **76**, 3510 (1996).
- [19] K. E. G. Löbner, M. Vetter, and V. Hönig, Nuclear Data Tables **A7**, 495 (1970).
- [20] T. Bengtsson and I. Ragnarsson, Nucl. Phys. **A436**, 14 (1985).
- [21] S. M. Mullins, J. Nyberg, A. Maj, M. S. Metcalfe, P. J. Nolan, P. H. Regan, R. Wadsworth, and R. A. Wyss, Phys. Lett. B **312**, 272 (1993).
- [22] D. Bazzacco *et al.*, Phys. Rev. C **49**, R2281 (1994).
- [23] R. Wyss and A. Johnson, in *Proceedings of the International Conference on High Spin Physics and Gamma-soft Nuclei*, edited by J. X. Saladin, R. A. Sorenson, and C. M. Vincent (World Scientific, Singapore, 1991), p. 123.
- [24] W. Satula, R. Wyss, and F. Dönau, Nucl. Phys. **A565**, 573 (1993).